

Hydrothermal Depolymerization of Lignin: Understanding the Structural Evolution

Jinxing Long, Ying Xu, Tiejun Wang, Riyang Shu, Qi Zhang*, Xiaohong Zhang, Juan Fu, and Longlong Ma

The structural evolution of *Panicum virgatum* lignin during hydrothermal depolymerization was investigated. Product distribution from various temperatures was studied using gas chromatography-mass spectrometry (GC-MS) and gel permeation chromatography (GPC) analysis. The physical-chemical properties of initial lignin, tetrahydrofuran soluble fraction, and char were also comparatively characterized by elemental analysis, scanning electron microscopy (SEM), thermogravimetry (TG), and Fourier transform infrared (FT-IR) spectroscopy. Results showed that both the depolymerization and repolymerization were significantly temperature-dependent. The undesired char formation becomes obvious when the temperature is greater than 180 °C. Further investigation demonstrated that H lignin is the most accessible for hydrothermal depolymerization, whereas S lignin is the most recalcitrant. Moreover, under the thermal effect and the dissolution of the subcritical water, the basic structure of lignin was first collapsed and then further decomposed into low-molecular weight products by the fracture of ether bonds, accompanied by char formation after repolymerization and dehydration.

Keywords: Lignin; Depolymerization; Repolymerization; Structural evolution

Contact information: Key Laboratory of Renewable Energy, Guangzhou Institute of Energy Conversion, Chinese Academy of Sciences, Guangzhou 510640, P. R. China;

*Corresponding author: zhangqi@ms.giec.ac.cn

INTRODUCTION

Lignin is a high potential feedstock for value-added chemicals and high quality biofuel because it is abundant, readily available, and renewable (Heitner *et al.* 2010). The conversion of this unique and natural aromatic polymer has attracted increasing attention during the last few decades because of the increasingly serious depletion of fossil fuels and associated environmental problems, such as the greenhouse effect and acid rain. Generally, pyrolysis, liquefaction, and gasification are efficient approaches to lignin conversion (Zakzeski *et al.* 2010; Zhang *et al.* 2014; Sameni *et al.* 2014). However, these processes are normally performed at high temperatures, resulting in high energy costs and low product quality. For example, the liquid products from pyrolysis exhibit several drawbacks, which include low energy density, high acid content, immiscibility with hydrocarbons, and wide variation in boiling point temperatures (Wildschut *et al.* 2009; Ansari and Gaikar 2014). Therefore, further treatment, such as upgrading, is necessary. Catalytic hydrogenation and oxidation are also proven to be suitable for lignin utilization (Zhang *et al.* 2011), but the addition of H₂ and oxidants results in obvious operational dangers and high equipment requirements. Furthermore, in general, H₂ currently originates from a fossil fuel, making it an unsustainable resource. Almost all of the reported processes lead to hard char formation, an undesired but inevitable byproduct during high-temperature depolymerization of

biomass. Therefore, intensive investigation of the structural evolution of lignin during thermal chemical processes is important and can provide a promising reference for efficient lignin utilization at mild conditions (*i.e.*, low temperature and pressure), especially for highly selective depolymerization and reduced char formation.

Green solvent water has been widely used in the chemical industry since it is readily available, cost-efficient, and has environmentally friendly properties. Hydrothermal depolymerization is also an efficient process for biomass utilization (Demirbas 2010; Moeller *et al.* 2011; Zhang *et al.* 2014). For example, Akhtar *et al.* (2010) reported that empty palm fruit bunches could be liquefied efficiently in alkaline hot compressed water, where more than 60.1% of liquid products were phenolic; however, aromatic bio-char was generated. We found that sugarcane bagasse, a typical agricultural residue in South China, could be liquefied efficiently under the catalysis of SO₃H-functionalized ionic liquids in subcritical water. More than 48% of volatile chemicals were obtained, but it also exhibited char formation from lignin (Long *et al.* 2011c). Hydrothermal decomposition of rapeseed straw in subcritical water has also been studied. Results showed that lignin is much more inflexible for decomposition than carbohydrates, and the residual solid consisted primarily of phenolic biochar (Pinkowska and Wolak 2013). Base-catalyzed depolymerization of Kraft lignin has been examined in near-critical water, where more than 17% of aromatic products were obtained. However, a 22% yield of biochar was also found (Nguyen *et al.* 2014).

As mentioned above, lignin is generally more recalcitrant than carbohydrates to conversion. Furthermore, its thermal decomposition is always accompanied by serious char generation, which significantly hampers further efficient utilization of this high-energy potential aromatic material. Subcritical water with a temperature of more than 200 °C can generate H₃O⁺ ions (Luo *et al.* 2007), so it is considered to be an excellent catalyst for acid catalytic processes. The *in situ* formation of the acid is reversible and the protons automatically disappear at ambient temperatures, leading to complete elimination of the problems of acid recovery and waste disposal (Chamblee *et al.* 2004; Luo *et al.* 2007). Therefore, we report here an efficient process for lignin depolymerization in environmentally benign solvent water at various temperatures. The primary target of this work is to provide a novel and promising method for future exploitation of lignin depolymerization technology with high products yield and char elimination through an intensive investigation of the internal structure change and chemical bonding crack.

EXPERIMENTAL

Materials

All chemical reagents were of analytical grade and used as received. Tetrahydrofuran (THF; HPLC grade), which was used as the eluent for gel permeation chromatography (GPC, Agilent 1260 HPLC; USA) analysis, was purchased from Acros Organics (Belgium). Other chemicals used in this study were all provided by Tianjin Chemical Co., Ltd. (China). *Panicum virgatum* was kindly donated by Prof. Jingjuan Yu (China Agricultural University). The organosolv lignin was separated according to a previously published procedure (Long *et al.* 2013), and the purity was determined by Fourier transform infrared (FT-IR) spectroscopy, proton nuclear magnetic resonance spectroscopy (¹H-NMR; *d*₆-dimethyl sulfoxide (DMSO) as solvent; Bruker Advance 400

III spectrometer, Switzerland), and dilute acid hydrolysis. Results showed that this material had high purity, with a residual sugar content lower than 2.81%.

Methods

Hydrothermal depolymerization of lignin

The depolymerization of lignin was carried out in a 100 mL stainless autoclave batch reactor equipped with a thermocouple, pressure transducer and gauge, jacketed electrical heating, and mechanical agitation device (Weihai Chemical Machinery Co., Ltd., Shandong, China). Typically, 1.0 g of lignin and 40 mL of deionized water were loaded into the reactor. After carefully displacing the air with N₂, the reactor was heated to 180 °C for 2 h. When the hydrothermal depolymerization was completed, the autoclave was cooled to room temperature in 20 min using flowing water. The mixture was removed and the reactor thoroughly washed with THF until solid and black viscous slime were not present.

Product separation and analysis

The mixture of lignin, depolymerized product, and biochar was separated according to the following procedure. After a series of filtration procedures, washing with THF three times (3×10 mL), and drying at 70 °C overnight under vacuum, the solid, designated as char, was collected and weighed to calculate the yield of char. Volatile products were extracted with CH₂Cl₂ from the water-soluble fraction, and their quality and quantity were determined using a gas chromatograph-mass spectrometer (GC-MS) and gas chromatography-flame ionization detector (GC-FID), respectively. The THF-soluble fraction, including phenolic oligomers from lignin hydrothermal depolymerization and the free feed lignin, was obtained by the careful removal of the solvent under reduced pressure.

The chemicals in the volatile fraction were determined on an Agilent 7890A GC with an Agilent 5975 mass-selective detector (USA) and identified according to the NIST MS library. An Agilent HP-INNOWax (30 m × 0.25 mm × 0.25 μm) capillary column was used for chemical separation with a split ratio of 5:1 and 99.999% helium as the carrier gas. The oven temperature was programmed as 60 °C (held 2 min), ramped up to 260 °C at 10 °C min⁻¹, and held for another 10 more min. The injector was kept at 280 °C. The contents of the volatile products were measured by the internal standard method on an Agilent 7890 GC with a FID detector (standard compound: acetophenone). The capillary column and temperature program were the same as for the GC-MS analysis.

The molecular weight distribution of the THF-soluble fraction was measured on an Agilent 1260 high-performance liquid chromatograph (HPLC, USA) with a differential refraction detector (RID). Tetrahydrofuran (HPLC-grade) was used as the eluent, with a flow rate of 1.0 mL min⁻¹. Polystyrene was used as the internal standard compound to determine the average molecular weight. The ¹H-NMR spectrum of this fraction was recorded on a Bruker Advance 400 III spectrometer (Switzerland), with deuterium dimethylsulfoxide (*d*₆-DMSO) as the solvent.

The elemental compositions of the THF-soluble fraction and char were determined by elemental analysis (Elementar Analysensysteme GmbH, vario EL III elemental analyzer; Germany). The oxygen content was estimated by the conservation of mass based on the assumption that the sample only contained C, H, N, S, and O. The physical properties of the THF-soluble fraction and char were characterized using a Hitachi S-4800 scanning electron microscope (SEM; Japan) and the chemical properties on a Linseis STA PT 1600 Thermogravimetric Analyzer (TG; Germany). For SEM, the samples were mounted on aluminum stubs, coated with gold (0.5 μm), and analyzed at an accelerating voltage of 20

kV. The TG temperature program was set from an initial temperature of 30 °C to a final temperature of 900 °C at the rate of 10 °C min⁻¹. The FT-IR spectra were acquired on a Nicolet iS™50 FT-IR spectrometer (USA) using the KBr pelleting method.

RESULTS AND DISCUSSION

Hydrothermal Depolymerization of Lignin

Table 1 summarizes the thermal decomposition of organosolv lignin in water with various temperatures and times. As our previous works (Long *et al.* 2011a,b,c; 2012) on biomass conversion have shown, this process is highly temperature-sensitive. The depolymerization became more significant with increasing reaction temperature, where the yield of volatile products increased, accompanying the obvious decrease in the THF-soluble fraction selectivity. For example, the highest yield of volatile chemicals of 9.28% and the lowest yield of THF soluble fraction of 19.84% were obtained at 250 °C. However, when this process was conducted at 160 °C, only 2.36% of lignin was converted to low-boiling point compounds, while most of it (62.54%) was dissolved by THF, as shown in Table 1. This conclusion is also in good accordance with the previous results obtained without catalysts, where temperature had a significant promotion effect on the yield of aromatic chemicals (Forchheim *et al.* 2012).

Table 1. Hydrothermal Depolymerization of Lignin^[a]

Temperature (°C)	Time (h)	Products distribution (%) ^[b]			
		Char	THF soluble ^[c]	Volatile products	Water soluble ^[d]
250	2	42.02	19.84	9.28	28.86
220	2	29.96	26.56	7.61	35.87
200	2	21.89	41.32	5.85	30.94
180	2	nd ^[e]	56.85	3.27	39.88
160	2	nd ^[e]	62.54	2.36	35.10
180	4	8.52	51.68	3.85	35.95
180	8	14.70	47.17	4.53	33.60

^[a] Lignin: 1.0 g; H₂O: 40 mL
^[b] The yield of the char and THF-soluble fraction were measured by weight comparison with the initial lignin; the yield of volatile products was determined by GC with acetophenone as the internal standard compound
^[c] Including the phenolic oligomer and the unconverted lignin
^[d] Estimated by the conservation of mass
^[e] nd: not detected

There are generally three continuous processes in lignin depolymerization, namely, its decomposition to phenolic oligomers, to trimers and dimers, and to phenolic monomers such as phenol, guaiacol, catechol, syringol, and their derivatives. Here, they are the main components of the THF-soluble, water-soluble, and volatile products, respectively. It is also reported that the thermal decomposition of lignin follows the free radical mechanism (Heitner *et al.* 2010). Generally, free radicals are much easier to generate at higher temperatures. Therefore, high-temperature depolymerization results in an obvious increase in volatile small molecules and a decrease in oligomers (Table 1). According to previous studies (Chamblee *et al.* 2004; Luo *et al.* 2007), H⁺ generation occurs when the water is hotter than 200 °C; at the same time, the lignin depolymerization process can be accelerated significantly with an acidic catalyst. This explains the sharp volatile product increase and

THF-soluble fraction decrease when the water temperature increased from 180 to 200 °C. Noticeably, Table 1 also demonstrates that obvious char formation occurred when the temperature was higher than 200 °C, and this tendency was more significant at elevated temperatures: for example, 42.02% of lignin was converted to char at 250 °C. According to previous studies (Have and Teunissen 2001; Long *et al.* 2014), the reformation of char is caused by the repolymerization of lignin and unsaturated oligomers, followed by dehydration on the surface. Both the decomposition and repolymerization processes follow the free radical mechanism and can be promoted remarkably by an acidic catalyst (Zakzeski *et al.* 2010). Furthermore, under elevated temperatures, the dehydration is more significant. Therefore, with increasing intensity of free radicals and the promotion of acid density and dehydration capability, the yield of char increased at high temperatures. Correspondingly, the lack of char at 180 and 160 °C can be attributed to weak repolymerization and dehydration (Table 1).

Compared with the temperature, the effect of time is insignificant. As shown in Table 1, 8.52% lignin was converted to char when the time was 4 h; however, no more than 14.70% of char generation even prolonged the time to 8 h at 180 °C. As discussed above, the low density of free radicals and non-generation of H_3O^+ ions may be responsible for this result. Certainly, the insignificant dehydration at this temperature is a primary reason for the lower char yield. The slight increase in the volatile product and the decrease of the THF-soluble fraction could be ascribed to efficient lignin decomposition.

GC-MS Analysis of the Volatile Products

The volatile chemicals were detected and identified by GC-MS. As shown in Fig. 1a and Table 2, the hydrothermal depolymerization of lignin is complex with respect to not only the process but also the product distribution. Phenol, guaiacol, syringol, and their derivatives, which normally originate from the decomposition of hydro-phenyl lignin (H-lignin), guaiacyl lignin (G-lignin), and syringyl lignin (S-lignin), respectively (Heitner *et al.* 2010), were detected, indicating that all structural units of lignin are convertible. However, the results listed in Table 2 also show that phenol and its derivatives are more abundant than the guaiacyl chemicals, while the syringyl compounds were few during the depolymerization process at various temperatures. According to a previous report, G, S, and H lignin are at an approximate ratio of 100:70:7 in grass biomass (Heitner *et al.* 2010). Therefore, the GC-MS results indicate that H lignin may more readily undergo decomposition than both G and S lignin. Interestingly, the selectivity of chemicals such as 4-ethyl phenol, a versatile compound from coumaric and ferulic acid of H lignin (Chatonnet *et al.* 1992, Gasson *et al.* 2012), decreased at elevated temperatures, especially at temperatures higher than 200 °C. This selectivity decrease of 4-ethyl phenol can be attributed to the abovementioned effect of temperature on free radicals and the self-generation of H_3O^+ by subcritical water. The GC-MS also detected two non-aromatic chemicals with retention times of 8.86 and 10.64 min; these were identified as furfural and ethyl levulinate, respectively. Generally, these compounds originate from the acid-catalyzed depolymerization of the lignin carbohydrate complex (LCC) section of lignin. Therefore, the sharp increase in the furfural content at 250 °C is attributed to acid generation by hot compressed water. The GC-MS analysis results demonstrated that lignin hydrothermal depolymerization was significantly temperature-dependent. At low temperatures, the products were more concentrated and the selectivity of the target chemicals was higher. Therefore, the exploitation of a novel and efficient catalytic process

for value-added aromatic chemicals such as 4-ethyl phenol would be important and essential for future lignin utilization.

Table 2. The 23 Most Abundant Aromatic Chemicals in the Volatile Products

NO	RT (min)	Chemical	Area percentage (%)				
			(160°C)	(180°C)	(200°C)	(220°C)	(250°C)
1	13.50	Phenol, 2-methoxy-	3.45	7.14	6.03	3.45	3.37
2	14.49	Phenol, 2-methoxy- 4-methyl-	1.73	5.36	3.65	3.34	1.98
3	14.96	Phenol, 2-methyl-	1.15	3.59	1.98	4.25	6.78
4	15.00	Phenol	3.51	7.94	6.32	1.09	3.23
5	15.23	Phenol, 4-ethyl-2- methoxy-	8.92	8.01	7.99	2.44	8.43
6	15.75	Phenol, 4-methyl-	1.40	5.40	3.09	1.19	1.93
7	16.62	Phenol, 4-ethyl-	27.26	16.54	18.89	20.03	22.19
8	17.45	Phenol, 2,6-dimethoxy-	2.63	5.77	5.49	4.60	2.65
9	18.20	Benzoic acid, 4-hydroxy-3-methoxy-	0.95	4.36	3.39	4.70	1.68
10	18.59	Benzofuran, 2,3-dihydro-	-	-	0.86	0.72	0.56
11	18.68	Benzene, 1,2,3-trim ethoxy-5-methyl-	1.12	2.27	1.88	3.28	1.37
12	20.07	Vanillin	1.58	2.56	1.30	2.09	1.35
13	20.59	Benzoic acid, 4-hydroxy -3-methoxy-, ethyl ester	3.31	2.12	2.56	4.13	2.75
14	20.69	Ethanone,1-(4-hydroxy- 3-methoxyphenyl)-	-	1.19	1.32	2.21	0.82
15	20.85	Benzeneacetic acid, 4-hydroxy- 3-methoxy-	4.92	4.97	5.41	4.13	4.15
16	22.29	Ethyl-.beta.-(4-hydroxy-3-methoxy-phenyl)-propionate	-	1.56	1.19	2.89	0.75
17	22.48	2,4'-Dihydroxy-3'-methoxyacetophenone	1.03	1.43	1.11	2.23	1.48
18	24.22	4-hydroxy-3,5-dimethoxy-Benzaldehyde	-	-	-	-	1.16
19	24.76	Ethylparaben	-	-	-	-	1.08
20	24.83	3,4,5-Trimethoxyphenylacetic acid	1.60	-	-	1.77	1.47
21	25.37	3,5-Dimethoxy-4-hydroxy phenylacetic acid	1.76	2.37	2.38	4.23	1.53
22	26.47	p-Hydroxycinnamic acid, ethyl ester	-	-	-	5.26	-
23	29.21	Ethyl (2E)-3-(4-hydroxy -3-methoxyphenyl)-2-propenoate	-	-	2.43	2.25	2.03
	Total		66.32	82.58	77.27	80.28	72.74

NO: the peak number listed in Fig.1a; **RT:** retention time; **Chemicals:** identified by GC-MS according to NIST MS library.

GPC and ¹H-NMR Analysis of the THF-soluble Fraction

Figure 1b shows the GPC analysis results of the THF-soluble fraction. The THF-soluble fraction from the depolymerization process at 160 °C exhibited almost the same GPC curve (Fig. 1b, curve b) as the raw material (Fig. 1b, curve a). This suggests that it is mostly composed of free feedstock because lignin decomposition is insignificant at this temperature, which also explained well the above result of scarce volatile product species and low contents (Tables 1 and 2, Fig. 1a). However, when the hydrothermal process was

carried out at 180 °C, an obvious increase in the average molecular weight and degree of dispersity was obtained because of the simultaneous depolymerization and repolymerization of lignin and the phenolic oligomer. At reaction temperatures above 180 °C, the repolymerization of the THF-soluble fraction became more significant, resulting in remarkable char formation and a decrease in not only the yield, but also the average molecular weight, of the THF-soluble fraction.

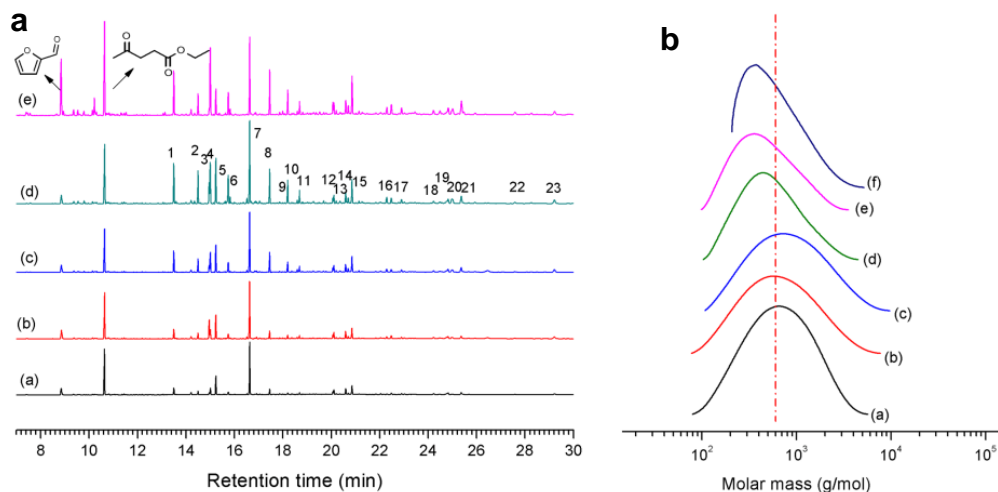


Fig. 1. (a) GC-MS analysis of volatile products and (b) GPC analysis of THF-soluble fraction at various temperatures.

GC-MS analysis: (a) 160 °C, (b) 180 °C, (c) 200 °C, (d) 220 °C, and (e) 250 °C.

GPC analysis: (a) initial lignin, and THF-soluble fraction from (b) 160 °C, (c) 180 °C, (d) 200 °C, (e) 220 °C, and (f) 250 °C

Proton NMR was used to further determine the structural evolution of the THF-soluble fraction (Fig. 2). The initial lignin exhibited the characteristic $^1\text{H-NMR}$ spectrum of grass biomass (Sun *et al.* 2003; Zhang *et al.* 2010). The strong signal at 3.74 ppm indicates the existence of abundant methoxy groups. The signals at 0.85 to 2.71 ppm are from the side-chain of the phenylpropane structure. This lignin also includes all of the H, G, and S units with characteristic chemical shifts at 6.74, 7.00, and 7.56 ppm, respectively (Long *et al.* 2015). Integral results demonstrated that the S/G/H ratio was 1/1.71/0.50. However, when it was treated by hot compressed water, the structure of lignin changed remarkably at various temperatures. For example, the main structure of lignin was not obviously changed at 160 °C due to the slight depolymerization, resulting in few volatile aromatic chemicals (Tables 1 and 2, Fig. 1a). The disappearance of signals at 3.45 and 7.56 ppm, which were from the H in the phenylcoumarane substructures and *p*-hydro-phenyl units, respectively, suggests efficient decomposition of the H-lignin. This also confirms the GC-MS analysis results suggesting that most of the volatile products were composed of phenol and its derivatives (Table 2). The strong signal at 3.36 ppm indicates that a large amount of phenolic monomers and oligomers are produced after depolymerization.

As discussed above, lignin was decomposed efficiently at 180 °C, with a large amount of volatile aromatic chemicals (Tables 1 and 2) and without char formation. Therefore, the $^1\text{H-NMR}$ spectrum of the THF-soluble fraction at 180 °C (Fig. 2c) was quite different from that of both the raw lignin (Fig. 2a) and the THF-soluble fraction at 160 °C (Fig. 2b). The sharp increase in the signal at 1.76 to 2.43 ppm clearly suggests the breakage of the lignin structure and an increase in alkyl groups directly attached to the aromatic ring. However, these groups are not the terminal because of their split peaks at 2.14 and 2.43

ppm. It is noteworthy that the appearance of new peaks at 4.27 and 5.07 revealed that the oligomer primarily originated from G lignin. This can be further shown by the G/S ratio measurement, which decreased from 1.71 for feedstock to 1.10 for this THF-soluble fraction. At further elevated temperatures, the lignin was more completely decomposed. Therefore, the THF-soluble fraction mostly consisted of phenolic oligomers, which showed different $^1\text{H-NMR}$ spectra (Figs. 2d through 2f). The free phenolic hydroxyl group was further increased with decreasing G/S ratio. The disappearance of signals at 3.61 and 4.13 ppm indicates the breakage of the $\beta\text{-O-4}$ bonds of lignin. However, the reappearance of signals at 5.02 and 4.06 ppm can be attributed to the repolymerization, which also contributes to the slight increase in the G/S ratio at 250 °C. Thus, the $^1\text{H-NMR}$ spectra of the THF-soluble fraction demonstrate that the H-lignin is more easily decomposed, followed by the G unit, whereas S lignin is the most difficult to decompose. The repolymerization of the oligomer is more significant when the temperature is above 200 °C. This conclusion agrees well with the GPC analysis (Fig. 1b).

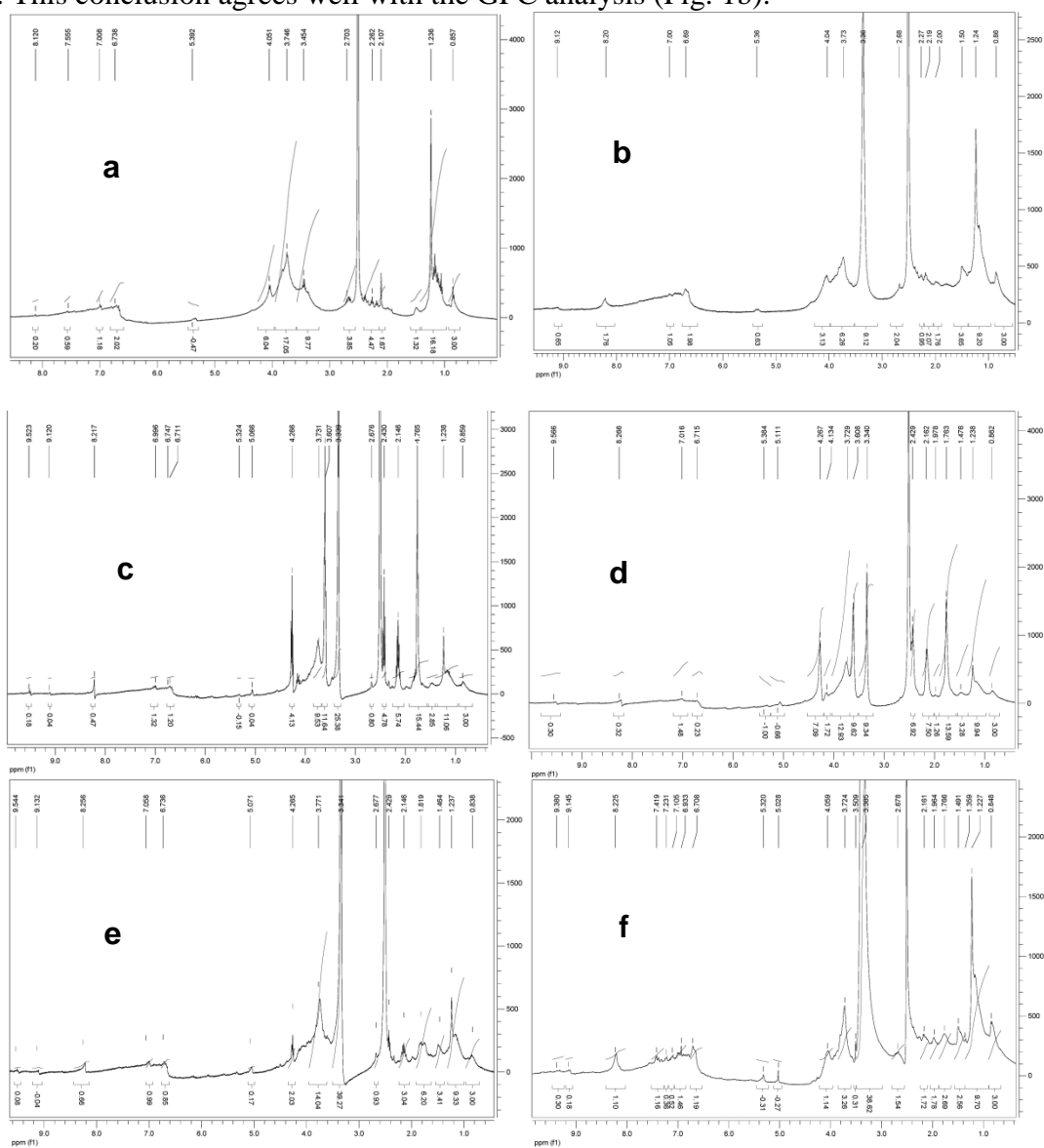


Fig. 2. $^1\text{H-NMR}$ analyses of (a) initial lignin and THF-soluble fraction at (b) 160 °C, (c) 180 °C, (d) 200 °C, (e) 220 °C, and (f) 250 °C

Elemental and SEM Analysis of THF-soluble Fraction and Char

Table 3 summarizes the elemental composition of initial lignin, the THF-soluble fraction from 160 to 180 °C, and the char from 200 to 250 °C. The initial lignin was composed of 65.32% C, 5.79% H, 27.75% O, 0.39% N, and 0.75% S, with a higher heating value (HHV) of 25.40 kJ kg⁻¹ and degree of unsaturation of 5.29. The THF-soluble fraction from 160 °C has almost the same C, H, O, and N contents, HHV, and degree of unsaturation as the raw material. The decrease of the S content is due to the decomposition of lignin-SO₃H, which originates from the lignin separation process with H₂SO₄ catalyst (Heitner *et al.* 2010). At 180 °C, the depolymerization is more significant, resulting in more volatile products and fewer oligomers (Table 1). The THF-soluble fraction from this temperature also showed a higher carbon content and HHV, with a lower degree of unsaturation because of the formation of the unsaturated aromatic chemicals, as detected by GC-MS and listed in Table 2. As for biochar, an increase in the C content and unsaturation was observed, with a decrease in the H and O contents. The dehydration of water at elevated temperatures may be responsible for this result. However, the elemental ingredients of biochar generated from this process are much more similar to the raw lignin than are those of other reported chars (Marquez-Montesinos *et al.* 2002), even at 250 °C. This indicates the incomplete carbonization of the repolymerization product of the oligomer and lignin.

Table 3. Elemental Analysis of Lignin and Residue at Various Temperatures^[a]

Temp. (°C)	Elemental content					Experimental molecular formula	HHV (KJ/kg) ^[c]	D ^[d]
	C	H	O ^[b]	N	S			
160	66.22	5.77	27.51	0.35	0.15	C ₉ H _{9.41} O _{2.80} N _{0.041} S _{0.008}	25.72	5.29
180	67.00	6.02	26.48	0.35	0.15	C ₉ H _{9.70} O _{2.67} N _{0.041} S _{0.008}	26.52	5.15
200	69.50	4.58	25.33	0.49	0.10	C ₉ H _{7.12} O _{2.46} N _{0.054} S _{0.005}	25.52	6.44
220	71.05	4.47	23.71	0.55	0.22	C ₉ H _{6.79} O _{2.25} N _{0.060} S _{0.010}	26.18	6.60
250	71.22	4.23	23.92	0.51	0.12	C ₉ H _{6.41} O _{2.27} N _{0.055} S _{0.006}	25.86	6.79
lignin	65.32	5.79	27.75	0.39	0.75	C ₉ H _{9.41} O _{2.87} N _{0.046} S _{0.039}	25.40	5.29

^[a]On a dry basis (sample was dried under vacuum at 80 °C until no further weight loss occurred)
^[b]The oxygen content was estimated by the conservation of mass based on the assumption that the samples only contained C, H, N, S, and O
^[c]Evaluated by the Dulong formula (Long *et al.* 2011c): HHV (MJ/kg) = 0.3383 × C + 1.422 × (H-O/8)
^[d]Degree of unsaturation

Scanning electron microscopy analysis was used to characterize the surface morphologies of the raw lignin, THF-soluble fraction from the depolymerization process at 180 °C, and char at 250 °C. As shown in Fig. 3, the surface of the original lignin was loose with an average particle diameter of about 200 nm (Fig. 3a). However, when lignin was treated with hot compressed water at 180 °C, the internal structure collapsed and the spherical particles completely disappeared, leaving a smooth, fused, and highly reflective surface (Fig. 3b). The significant changes to the surface can be attributed to three main issues: (1) the hydrothermal swelling effect of solvent on the lignin, (2) the breakage of the connected chemical bonding of lignin molecules such as β-O-4 and 4-O-5, *i.e.*, the depolymerization of lignin, which promotes the collapse of the lignin structure, and (3) the recombination of the chemical bonds of lignin, *i.e.*, repolymerization of phenolic oligomers and lignin, resulting in the reconfiguration of the lignin surface. When the lignin was hydrothermally depolymerized at 250 °C, the surface of the char was altered, showing a

typical coke surface (Fig. 3c), a loose and porous coating of black particles with diameters of no more than 100 nm. Incompletely dehydrated lignin and tar can also be observed. Therefore, the SEM images revealed that lignin first swelled with the collapse of the internal support structure, *e.g.*, hydrogen bonds, leading to a homogenous fused and pitch-like substance. Then, under the thermal effect, the active chemical ester bonds of this pitch-like substance, such as β -O-4 and 4-O-5, were cracked, giving volatile aromatic products and oligomers. The unsaturated aromatic oligomers can also repolymerize under the same condition to provide the undesired solid. Simultaneous depolymerization and repolymerization therefore contributes to the smooth and highly reflective surface. The repolymerization product is more chemically and thermally stable than the feedstock. However, dehydration is prevalent at high temperatures, resulting in the alveolate surface.

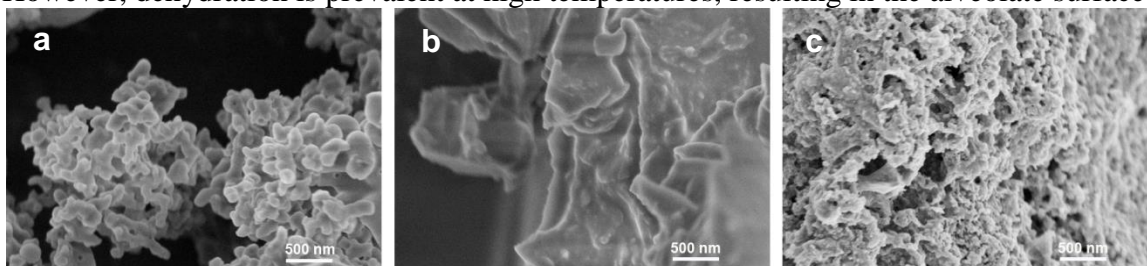


Fig. 3. SEM images of (a) raw lignin, (b) THF soluble fraction at 180 °C, and (c) char at 250 °C

TG and FT-IR Analysis

Thermogravimetric analysis is a powerful method for determining the structural evolution and thermal decomposition of biomass and depolymerization residue (Serrano *et al.* 2010; Long *et al.* 2011b). Figure 4a shows that the onset decomposition temperature (T_{onset}) of the initial lignin was 215 °C, and a sharp weight loss was observed in the temperature range from 250 to 500 °C due to the efficient break of the active chemical bonds. It also decomposed gradually at elevated temperatures, leaving about 37.3 wt% of non-volatile residue. The THF-soluble fraction from 180 °C had almost the same thermal degradation properties as the original lignin. The decreased T_{onset} and quick weight loss at 150 to 240 °C (Fig. 4a, curve b) can be attributed to the loose and partly degraded structure caused by hydrothermal swelling and depolymerization, as discussed above. However, when the lignin was treated at 250 °C, the thermal decomposition properties of the residual solid were noticeably different (Fig. 4a, curve c). The T_{onset} markedly increased, with more than 59 wt% of the raw material remaining, and was non-volatilized, even at 900 °C, due to the formation of the highly condensed aromatic coke. This suggests that the char is also composed of lignin and oligomers. The surface of this material was first carbonized, giving a coke-like surface morphology (Fig. 3c) and high T_{onset} (Fig. 4a, curve c). Under elevated temperatures, this char could be further degraded, which confirmed that the char had an elemental composition much more similar to the raw lignin than to other reported chars (Table 3).

The FT-IR was adopted to characterize the structural evolution of lignin during the hydrothermal depolymerization process. Figure 4b shows the FT-IR spectra of the original lignin and the residual solids. The strong absorption at 3418 cm^{-1} can be assigned to the stretching of phenolic OH. Peaks at 2931 and 2863 cm^{-1} can be attributed to the stretching vibration of OCH_3 and CH_2 , respectively (Mayo *et al.* 2004); C=O showed a strong absorption peak at 1707 cm^{-1} (Sun *et al.* 2014). The peaks at 1608, 1511, and 1458 cm^{-1} can be assigned to the characteristic vibrations of the benzene structures in lignin. The appearance of peaks at 1367 and 921 cm^{-1} indicate the existence of lignin carbohydrate

complex (LCC) (Mayo *et al.* 2004; Heitner *et al.* 2010). The peaks at 1268, 1215, 1117, and 1029 cm^{-1} represent the stretching breathing of Ar-O, where the peak at 1268 cm^{-1} is considered to be the characteristic absorption of G lignin and the one at 1117 cm^{-1} corresponds to the characteristic vibrations of the S unit (Wen *et al.* 2014, Chen *et al.* 2014). The peak at 836 cm^{-1} is associated with the out-of-plane vibration breathing of aromatic C-H (Mayo *et al.* 2004).

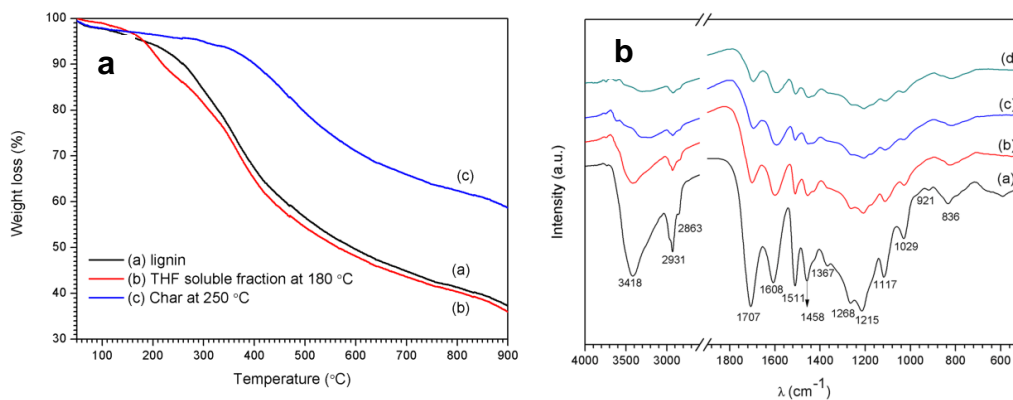


Fig. 4. (a) TG and (b) FT-IR analysis of initial lignin and residues: TG: (a) lignin; (b): THF-soluble fraction at 180 °C; and (c) char at 250 °C; FT-IR: (a) lignin; (b) char at 200 °C; (c) char at 220 °C; and (d) char at 250 °C

As shown in Fig. 4b, the FT-IR spectrum of biochar changed noticeably in comparison to the initial lignin. The gradual weakness of the peak strength at 3418 cm^{-1} indicated the depolymerization of lignin to phenolic monomers and oligomers. Certainly, the efficient dehydration at high temperatures also contributed to the -OH reduction. The strength decrease and the slight red shift of C=O suggests that ester cracking and carboxyl formation occurred with the formation of the chemicals containing C=O, as listed in Table 2. The complete disappearance of the peaks at 1367 and 921 cm^{-1} indicates that the LCC fraction is much more easily converted than the aromatic lignin. These results are in accordance with the GC-MS (Table 1) and $^1\text{H-NMR}$ (Fig. 2) results. Furthermore, the weak but obvious -OCH₃ and aromatic ring characteristic absorptions of Fig. 4b, curve (d) clearly demonstrate the original lignin structure. Moreover, compared with the S unit (1117 cm^{-1}), the absorption strength of G lignin (1268 cm^{-1}) was reduced noticeably at elevated temperatures. Therefore, FT-IR further confirms that the LCC part of lignin is more favorable to be converted than the aromatic structures. Among the three structural units of lignin, H lignin is the easiest to degrade, followed by G lignin, whereas S lignin is the most recalcitrant in the hydrothermal environment. The FT-IR results also demonstrated that the residual solid is partly carbonized, while still retaining the characteristic structure of lignin.

CONCLUSIONS

1. Lignin can be converted efficiently to useful aromatic products in hot compressed water. However, when the temperature is above 180 °C, the repolymerization and dehydration of phenolic oligomers become more significant, resulting in undesired biochar.
2. Further investigation demonstrated that H lignin is the most accessible for hydrothermal depolymerization, whereas S lignin is the most recalcitrant.
3. The depolymerization product is more selective at lower temperatures.

- Intensive analyses of the volatile and nonvolatile products and a comparison of the raw lignin, THF-soluble fraction, and char demonstrated that lignin depolymerization involved a continuous process of swelling, structural collapse, chemical bond breakage and transfer, repolymerization, and carbonization. All of these processes can be accelerated by the acid catalyst.

ACKNOWLEDGMENTS

The authors gratefully acknowledge the financial support of the Natural Science Foundation of China (No. 51036006, 51306191), the National Key Technology R&D Program (NO. 2014BAD02B01), and the National Basic Research Program of China (973 program, No. 2012CB215304).

REFERENCES CITED

- Akhtar, J., Kuang, S. K., and Amin, N. S. (2010). "Liquefaction of empty palm fruit bunch (EPFB) in alkaline hot compressed water," *Renew. Energ.* 35(6), 1220-1227. DOI: 10.1016/j.renene.2009.10.003
- Ansari, K. B., and Gaikar, V. G. (2014). "Pressmud as an alternate resource for hydrocarbons and chemicals by thermal pyrolysis," *Ind. Eng. Chem. Res.* 53(5), 1878-1889. DOI: 10.1021/ie401961y
- Chamblee, T. S., Weikel, R. R., Nolen, S. A., Liotta, C. L., and Eckert, C. A. (2004). "Reversible in situ acid formation for [small beta]-pinene hydrolysis using CO₂ expanded liquid and hot water," *Green Chem.* 6(8), 382-386. DOI: 10.1039/B400393D
- Chatonnet, P., Dubourdie, D., Boidron, J., and Pons, M. (1992). "The origin of ethylphenols in wines," *J. Sci. Food Agric.* 60(2), 165-178. DOI: 10.1002/jsfa.2740600205
- Chen, Y., Stark, N. M., Cai, Z., Frihart, C. R., Lorenz, L. F., and Ibach, R. E. (2014). "Chemical modification of kraft lignin: Effect on chemical and thermal properties," *BioRes.* 9(3), 5488-5500.
- Demirbas, A. (2010). "Sub- and super-critical water depolymerization of biomass," *Energ. Source. A* 32(12), 1100-1110. DOI: 10.1080/15567030802606111
- Forchheim, D., Hornung, U., Kempe, P., Kruse, A., and Steinbach D. (2012). "Influence of RANEY Nickel on the Formation of Intermediates in the Degradation of Lignin," *Int. J. Chem. Eng.* Article ID 589749, 8 pages, DOI:10.1155/2012/589749.
- Have, R., and Teunissen, P. J. M. (2001). "Oxidative mechanisms involved in lignin degradation by white-rot fungi," *Chem. Rev.* 101(11), 3397-3413. DOI: 10.1021/cr000115l
- Heitner, C., Dimmel, D., and Schmidt, J. (2010). *Lignin and Lignans: Advances in Chemistry*, CRC Press, Boca Raton, FL. DOI: 10.1201/EBK1574444865
- Gasson, R. J., Forchheim, D., Sutter, T., Hornung, U., Kruse, A. and Barth, T. (2012). "Modeling the Lignin Degradation Kinetics in an Ethanol/Formic Acid Solvolysis Approach. Part 1. Kinetic Model Development," *Ind. Eng. Chem. Res.* 51(32), 10595-10606. DOI: 10.1021/ie301487v.
- Long, J. X., Guo, B., Li, X. H., Wang, F. R., and Wang, L. F. (2011a). "Catalytic

- decomposition of cellulose in cooperative ionic liquids,” *Acta Phy. Chim. Sin.* 27(5), 995-999. DOI: 10.3866/PKU.WHXB20110506
- Long, J., Guo, B., Li, X., Jiang, Y., Wang, F., Tsang, S. C., Wang, L., and Yu, K. M. K. (2011b). “One step catalytic conversion of cellulose to sustainable chemicals utilizing cooperative ionic liquid pairs,” *Green Chem.* 13(9), 2334-2338. DOI: 10.1039/c1gc15597k
- Long, J., Guo, B., Teng, J., Yu, Y., Wang, L., and Li, X. (2011c). “SO₃H-functionalized ionic liquid: Efficient catalyst for bagasse liquefaction,” *Bioresour. Technol.* 102(21), 10114-10123. DOI: 10.1016/j.biortech.2011.08.043
- Long, J., Li, X., Guo, B., Wang, F., Yu, Y., and Wang, L. (2012). “Simultaneous delignification and selective catalytic transformation of agricultural lignocellulose in cooperative ionic liquid pairs,” *Green Chem.* 14(7), 1935-1941. DOI: 10.1039/C2GC35105F
- Long, J., Li, X., Guo, B., Wang, L., and Zhang, N. (2013). “Catalytic delignification of sugarcane bagasse in the presence of acidic ionic liquids,” *Catal. Today*, 200, 99-105. DOI: 10.1016/j.cattod.2012.08.018
- Long, J., Zhang, Q., Wang, T., Zhang, X., Xu, Y., and Ma, L. (2014). “An efficient and economical process for lignin depolymerization in biomass-derived solvent tetrahydrofuran,” *Bioresour. Technol.* 154, 10-17. DOI: 10.1016/j.biortech.2013.12.020
- Long, J., Lou, W., Wang, L., Yin, B., and Li, X. (2015). “[C₄H₈SO₃Hmim]HSO₄ as an efficient catalyst for direct liquefaction of bagasse lignin: Decomposition properties of the inner structural units,” *Chem. Eng. Sci.* 122, 24-33. DOI: 10.1016/j.ces.2014.09.026
- Luo, C., Wang, S., and Liu, H. (2007). “Cellulose conversion into polyols catalyzed by reversibly formed acids and supported ruthenium clusters in hot water,” *Angew. Chem. Int. Ed.* 46(40), 7636-7639. DOI: 10.1002/ange.200702661
- Marquez-Montesinos, F., Cordero, T., Rodriguez-Mirasol, J., and Rodriguez, J. J. (2002). “CO₂ and steam gasification of a grapefruit skin char,” *Fuel* 81(4), 423-429. DOI: 10.1016/S0016-2361(01)00174-0
- Mayo, D. W., Miller, F. A., and Hannah, R. W. (2004). *Course Notes on the Interpretation of Infrared and Raman Spectra*. John Wiley and Sons, Hoboken, NJ. DOI: 10.1002/0471690082
- Moeller, M., Nilges, P., Harnisch, F., and Schroeder, U. (2011). “Subcritical water as reaction environment: Fundamentals of hydrothermal biomass transformation,” *ChemSusChem* 4(5), 566-579. DOI: 10.1002/cssc.201000341
- Nguyen, T. D. H., Maschietti, M., Belkheiri, T., Amand, L. E., Theliander, H., Vamling, L., Olausson, L., and Andersson, S. I. (2014). “Catalytic depolymerisation and conversion of Kraft lignin into liquid products using near-critical water,” *J. Supercrit. Fluid.* 86, 67-75. DOI: 10.1016/j.supflu.2013.11.022
- Pinkowska, H., and Wolak, P. (2013). “Hydrothermal decomposition of rapeseed straw in subcritical water. Proposal of three-step treatment,” *Fuel* 113, 340-346. DOI: 10.1016/j.fuel.2013.05.088
- Sameni, J., Krigstin, S., Rosa, D. S., Leao, A., and Sain, M. (2014). “Thermal characteristics of lignin residue from industrial processes,” *BioRes.* 9(1), 725-737.
- Serrano, L., Egues, I., Alriols, M. G., Llano-Ponte, R., and Labidi, J. (2010). “*Miscanthus sinensis* fractionation by different reagents,” *Chem. Eng. J.* 156(1), 49-55. DOI: 10.1016/j.cej.2009.09.032

- Sun, J. X., Sun, X. F., Sun, R. C., Fowler, P., and Baird, M. S. (2003). "Inhomogeneities in the chemical structure of sugarcane bagasse lignin," *J. Agric. Food Chem.* 51(23), 6719-6725. DOI: 10.1021/jf034633j
- Sun, Y. C., Lin, Z., Peng, W.-X., Yuan, T. Q., Xu, F., Wu, Y. Q., Yang, J., Wang, Y. S., and Sun, R. C. (2014). "Chemical changes of raw materials and manufactured binderless boards during hot pressing: Lignin isolation and characterization," *BioRes.* 9(1), 1055-1071.
- Wen, J. L., Yuan, T. Q., Sun, S. L., Xu, F., and Sun, R. C. (2014). "Understanding the chemical transformations of lignin during ionic liquid pretreatment," *Green Chem.* 16(1), 181-190. DOI: 10.1039/C3GC41752B
- Wildschut, J., Mahfud, F. H., Venderbosch, R. H., and Heeres, H. J. (2009). "Hydrotreatment of fast pyrolysis oil using heterogeneous noble-metal catalysts," *Ind. Eng. Chem. Res.* 48(23), 10324-10334. DOI: 10.1021/ie9006003
- Zakzeski, J., Bruijninx, P. C. A., Jongerius, A. L., and Weckhuysen, B. M. (2010). "The catalytic valorization of lignin for the production of renewable chemicals," *Chem. Rev.* 110(6), 3552-3599. DOI: 10.1021/cr900354u
- Zhang, X. M., Yuan, T. Q., Peng, F., Xu, F., and Sun, R. C. (2010). "Separation and structural characterization of lignin from hybrid poplar based on complete dissolution in DMSO/LiCl," *Sep. Sci. Technol.* 45(16), 2497-2506. DOI: 10.1080/01496391003793892
- Zhang, X., Tu, M., and Paice, M. G. (2011). "Routes to potential bioproducts from lignocellulosic biomass lignin and hemicelluloses," *Bioenerg. Res.* 4(4), 246-257. DOI: 10.1007/s12155-011-9147-1
- Zhang, X., Zhang, Q., Long, J., Xu, Y., Wang, T., Ma, L., and Li, Y. (2014). "Phenolics production through catalytic depolymerization of alkali lignin with metal chlorides," *BioRes.* 9(2), 3347-3360.
- Zhang, Z., Lu, Q., Ye, X., Xiao, L., Dong, C., and Liu, Y. (2014). "Selective production of phenolic-rich bio-oil from catalytic fast pyrolysis of biomass: Comparison of K_3PO_4 , K_2HPO_4 , and KH_2PO_4 ," *BioRes.* 9(3), 4050-4062.

Article submitted: July 16, 2014; Peer review completed: September 30, 2014; Revisions accepted: October 7, 2014; Published: October 13, 2014.